  Bull. Chem. Soc. Jpn., 57, 627—633 (1984)

The Intermolecular Interaction of Tetrathiafulvalene and Bis(ethylenedithio)-tetrathiafulvalene in Organic Metals. Calculation of Orbital Overlaps and Models of Energy-band Structures

Takehiko MORI,* Akiko KOBAYASHI, Yukiyoshi SASAKI, Hayao KOBAYASHI,† Gunzi SAITO,†† and Hiroo INOKUCHI††

Department of Chemistry, Faculty of Science, The University of Tokyo, Hongo, Bunkyo-ku, Tokyo 113

†*Department of Chemistry, Faculty of Science, Toho University, Funabashi, Chiba 274*

††*Institute for Molecular Science, Okazaki 444*

(Received May 12, 1983)

Based on the extended Hückel molecular orbital calculations, the relation between the anisotropy of the band structure and the arrangement of the organic molecules is investigated for two organic donors, tetrathiafulvalene (TTF) and bis(ethylenedithio)tetrathiafulvalene (BEDT-TTF). The intermolecular overlaps of their HOMO are calculated while the intermolecular arrangements are varied. The maps of the overlaps thus obtained are then used to estimate the band-structure parameters of $(TMTTF)_2X$ and $(BEDT\text{-}TTF)_2ClO_4(C_2H_3Cl_3)_{0.5}$. The Fermi surface of $(TMTTF)_2X$ is quasi-one-dimensional and not closed. On the contrary, $(BEDT\text{-}TTF)_2ClO_4(C_2H_3Cl_3)_{0.5}$ is regarded as a two-dimensional semimetal.

It has been widely believed that a face-to-face stacking of planar molecules is an indispensable requirement of organic metals and that most of organic metals are quasi-one-dimensional conductors. In these compounds, the intermolecular π-π interaction is responsible for their one-dimensional energy band. However, charge- and spin-density-wave instabilities inherent in one-dimensional metals tend to destroy the metallic states. In the organic superconductors $(TMTSF)_2X$ (TMTSF; tetramethyltetraselenafulvalene, X=PF_6, AsF_6, SbF_6, ClO_4, *etc.*), however, it has been pointed out that the metallic states are stabilized by the relatively large transverse interaction.[1,2] Molecular orbital calculations using seiempirical parameters (extended Hückel method) have been performed by different authors for the $(TMTSF)_2X$ series compounds. Whangbo *et al.*,[3] Grant,[4] and the present authors[5] obtained a quasi-one-dimensional Fermi surface, at least when selenium 4 d orbitals were not included in the calculation. In these calculations, the ratio of the transverse and the longitudinal transfer integrals t_b/t_a was about 0.1. Including selenium 4d orbitals, Whangbo *et al.* noticed a large enhancement of the transverse dispersion leading to a closed Fermi surface on the a* b* plane. However, we found that the change in t_b/t_a was too small to close the Fermi surface. Minot and Louie obtained a complicated semimetallic band structure, with closed Fermi surfaces, by using 'swelled' selenium 4p orbitals, but no 4d orbital.[6] We obtained a similar result when the ionization potential of selenium 4d atomic orbitals was chosen close to the energy level of the highest occupied molecular orbital (HOMO).

On the other hand, increasing interest has been taken in the cation radical salts of BEDT-TTF (4,5-4',5'-bis(ethylenedithio)tetrathiafulvalene). Saito *et al.* reported that the conductivity of $(BEDT\text{-}TTF)_2ClO_4(C_2H_3Cl_3)_{0.5}$ is metallic down to 16 K; below this temperature it decreases slightly, but remains high (670 Ω^{-1} cm^{-1}) even at 1.4 K.[7] The X-ray structure analysis showed that this compound does not have the column structure characteristic of one-dimensional organic conductors.[8] We have calculated the intermolecular overlap integrals of this compound and showed the importance of the transverse interactions.[9] Recently it has also been observed that, in β-$(BEDT\text{-}TTF)_2PF_6$, which shows metal-insulator transition at 297 K, the most conducting axis is parallel to the molecular plane.[10] These results suggest that, in BEDT-TTF compounds, the transverse interaction is more important than, or at least is similar in importance to, the longitudinal interaction.

The present investigation is intended to clarify the relation between the anisotropy (dimensionality) of the band structure and the mode of the intermolecular arrangement of organic molecules. In the calculation, the methyl groups of TMTSF can be replaced by hydrogens (TSF; tetraselenafulvalene) without any significant change in the molecular orbitals. However, if its selenium atoms are replaced by sulfur (TTF; tetrathiafulvalene), the subsequent significant contraction of the atomic orbitals influences the molecular orbitals. In the present investigation, the calculation is performed for two organic donors, TTF and BEDT-TTF.

In order to discuss the physical properties on the basis of quantum-chemical calculations, it is necessary to

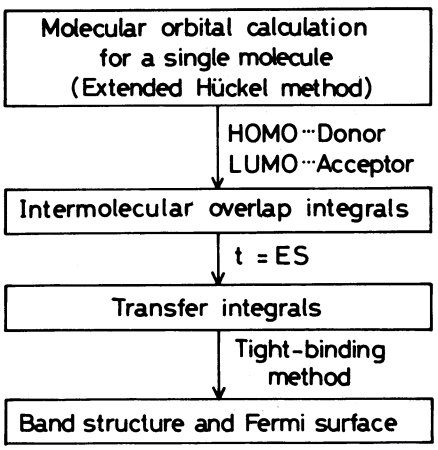

Scheme

carry out an energy-band calculation which takes the three-dimensional periodicity of the crystal into consideration. However, it is not easy to calculate the energy-band structure considering all electrons because of the large size of the organic molecules and because of the complicated crystal structures. Since the anisotropy of the physical properties mainly reflects the shape of the Fermi surface, we may neglect the levels other than the conduction level. Our procedure of the approximate band-structure calculation is thus (Scheme);

(1) Since the size of the organic molecules is very large, the molecular orbitals of a single molecule are calculated by means of the extended Hückel method.

(2) In the case of donor molecules, the intermolecular overlap S of the HOMO is calculated.

(3) Transfer integrals t are estimated using the relation $t=ES$, where E is a constant of the order of energy of the HOMO. This relation is the same as that generally used in the extended Hückel method to obtain resonance integrals.

(4) Using the standard tight-binding approximation, the band structure of the conduction band and the shape of the Fermi surface are obtained.

Alternatively, the transfer integrals can be obtained by calculating the molecular orbitals of a dimer. Unlike this method, our approximation completely neglects the polarization of the molecular orbitals caused by the interaction with other molecules. However, the simplicity of the calculation is more efficient in comparing a number of different intermolecular arrangements. In the present investigation, the intermolecular overlaps of the HOMO are calculated while the molecular arrangements are varied. Using the maps of the intermolecular overlaps thus obtained, the band-structure parameters of $(TMTTF)_2X$ and $(BEDT\text{-}TTF)_2ClO_4(C_2H_3Cl_3)_{0.5}$ are estimated, and the shape of their Firmi surface is discussed. In addition, the characteristic side-by-side arrangement of BEDT-TTF molecules in $(BEDT\text{-}TTF)_2ClO_4(C_2H_3Cl_3)_{0.5}$ is interpreted in view of the electronic stabilization due to the maximum overlap of the conduction orbitals.

Molecular Orbital Calculation

The molecular structures of TTF and BEDT-TTF were idealized so as to have a D_{2h} symmetry, based on the crystal structures of TTF-TCNQ and $(BEDT\text{-}TTF)_2ClO_4(C_2H_3Cl_3)_{0.5}$ (Fig. 1).[8,11] All the atoms except the hydrogens in BEDT-TTF were put on the xy-plane, and the x-axis was placed so as to correspond with the long axis of the molecule. The C-H bond lengths were assumed to be 1 Å.

Since the large size of the molecules prevented us from adopting *ab initio* calculations, the simple extended Hückel method was used. The parameters (Table 1) were taken from Ref. 12.

The coefficients of the HOMO are shown in Table 2. The HOMO of BEDT-TTF as well as that of TTF has a π-character with B_{1u} symmetry (in the D_{2h} point group) and has nodes on all the C-S bonds. The electron density is largest on the inner sulfur atom, S_1. The fact that the charge density on the outer sulfur atom, S_2, of BEDT-TTF is larger than the charge on the C_2 of TTF, shows the considerable expansion of the HOMO of BEDT-TTF in comparison with TTF.

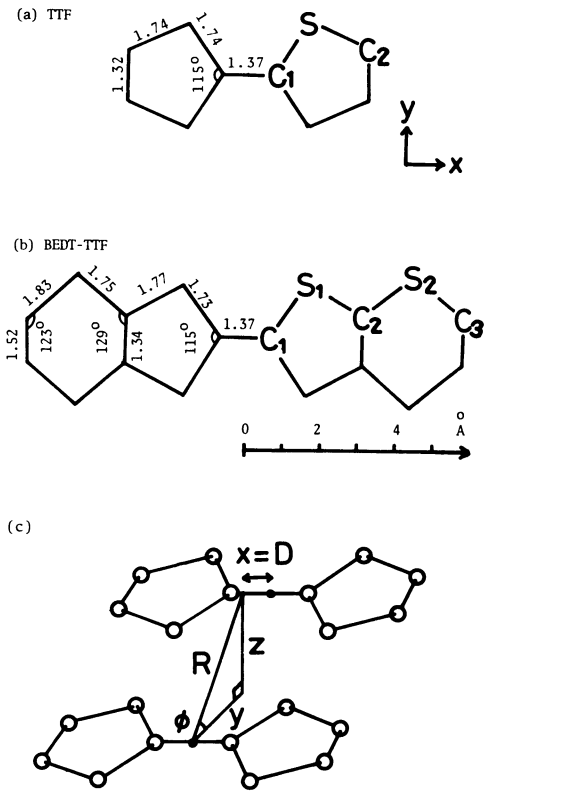

Fig. 1. Molecular structures of (a) TTF and (b) BEDT-TTF. Bond lengths in Å. (c) Relative orientation of a molecular dimer. D represents the molecular slipping along the long axis, R stands for the distance between the long axes of the two molecules, and ϕ is changed from 0° (the side-by-side arrangement) to 90° (the face-to-face stacking).

Table 1. The exponents ζ and the ionization energies ε (eV) for atomic orbitals

Atomic	Orbitals	ζ	ε
S	3 s	2.122	−20.0
	3 p	1.827	−11.0
	3 d	1.5	−5.44
C	2 s	1.625	−21.4
	2 p	1.625	−11.4
H	1 s	1.0	−13.6

Intermolecular Overlaps

Since, both in the $(TMTTF)_2X$ analogs and in many BEDT-TTF salts, molecules are arranged so as to keep their long axes and their molecular planes parallel to each other, we did not consider the relative rotation of the molecules. The relative arrangement of two molecules is represented by a set of cylindrical coordinates

Table 2. Coefficients of the highest occupied orbitals

TTF			BEDT-TTF		
C_1	$2p_z$	−0.26614	C_1	$2p_z$	−0.23510
S	$3p_z$	0.45070	S_1	$3p_z$	0.41358
	$3d_{yz}$	0.12960		$3d_{yz}$	0.12596
	$3d_{xy}$	−0.00412		$3d_{xy}$	−0.00498
C_2	$2p_z$	−0.13851	C_2	$2p_z$	−0.15968
			S_2	$3p_z$	0.16581
				$3d_{yz}$	0.06339
				$3d_{xy}$	0.01547
			C_3	$2p_z$	−0.01877
			H	1 s	0.00927

(D, R, ϕ), as is shown in Fig. 1 (c).

The molecular orbital calculation of a dimer when ϕ=90° has been repeatedly carried out for TCNQ and TTF as a function of D, in which attention has been paid to the most favored slipping D of the stacked molecules.[13] The total energy of a dimer may be divided into the core repulsion and the electronic bonding energy. In the case of TCNQ, the core repulsion is a flat function of D over a wide range of D, and the maximum of the overlap of the lowest unoccupied molecular orbitals (LUMO) corresponds with the minimum of the total energy and also agrees with the slipping in the actual crystals.[13,14] On the contrary, in the case of TTF, the actual slipping corresponds with the minimum of the core repulsion, and the overlap of the HOMO has a *minimum* near this slipping. The applica-

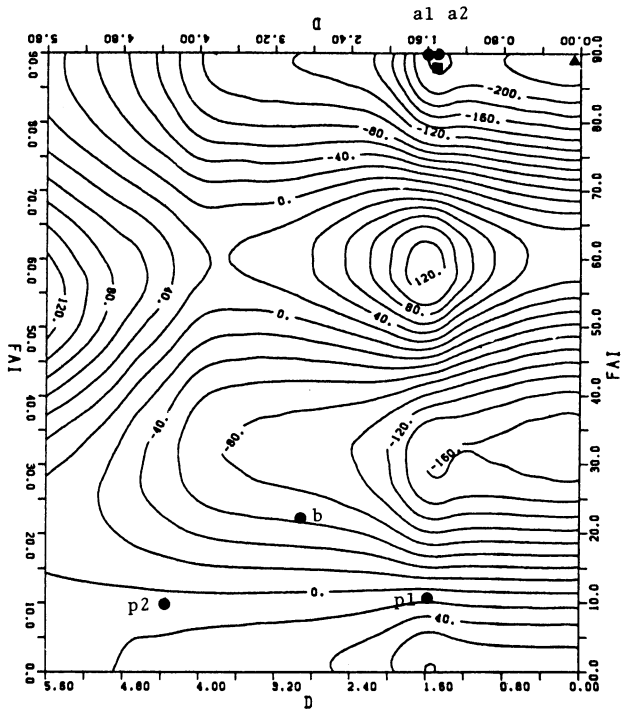

Fig. 2. Overlap integral ($\times 10^{-4}$) of the HOMO between two TTF molecules as a function of the slipping D and the relative angle ϕ (FAI) (see Fig. 1(c)). The triangle designates the stacking mode in TTF-$I_{0.72}$ or TTF-$SCN_{0.58}$. The aquare shows the slipping in the TTF-TCNQ analogs. The other symbols correspond to the interactions in $(TMTTF)_2X$ shown in Fig. 5.

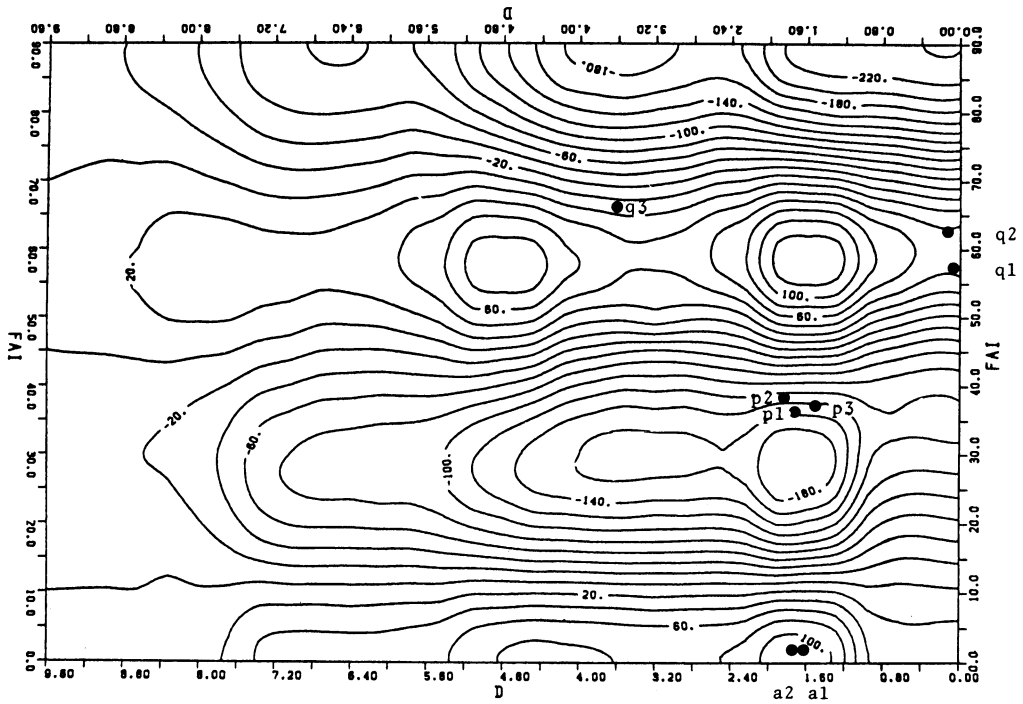

Fig. 3. Overlap integral ($\times 10^{-4}$) of the HOMO between two BEDT-TTF molecules as a function of the slipping D and the relative angle ϕ(FAI).
The symbols a1, a2, *etc.* correspond to the interactions in $(BEDT\text{-}TTF)_2ClO_4$ $(C_2H_3Cl_3)_{0.5}$ shown in Fig. 6.

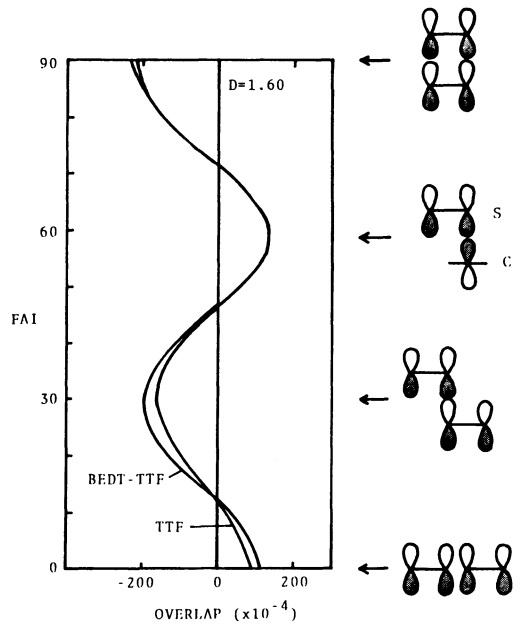

Fig. 4. Cross section of Figs. 2 and 3 at $D=1.60$ Å. In the right hand, the HOMO viewed along the long axes of the molecules are shown.

tion of the local-density-functional theory also suggests the importance of the core repulsion.[15] These results are not surprising, for the van der Waals radius of sulfur is considerably larger than those of carbon and nitrogen. In order to eliminate the effect of this core repulsion, we restricted our calculation to the plane of a crumpled cylinder where the shortest sulfur-to-sulfur distance was arbitrarily fixed as 3.80 Å. The effect of changing the sulfur-to-sulfur distance will be discussed later. By this 'rigid-body approximation,' the coordinate R is given as a function of the other two coordinates, D and ϕ.

In Figs. 2 and 3, the intermolecular overlap integrals are shown as a function of D and ϕ. Figure 4 shows the cross-section of Figs. 2 and 3 at $D=1.60$ Å. The largest overlap at $\phi=90°$ corresponds to the normal face-to-face stacking. The interaction at $\phi=0°$ is the π-like interaction of the p_z (and d) orbitals. The peak around $\phi=30°$ corresponds to the σ-like interaction. In these contexts, σ-like and π-like represent the overlaps which mainly come from the components of the p_z orbitals projected parallel to and perpendicular to the bonding direction respectively. The peak at $\phi=60°$, $D=1.60$ Å, mainly comes from the overlap between the central carbon, C_1, and the sulfur.

The interactions of the TMTTF molecules in $(TMTTF)_2Br$ are shown in Fig. 2 by five symbols, a_1, a_2, p_1, p_2, and b, which correspond to the interactions designated in Fig. 5.[16] Other $(TMTTF)_2X$ type compounds are isostructural to $(TMTTF)_2Br$, regardless of X. The longitudinal interactions, a_1 and a_2, are the same as that of TTF in TTF-TCNQ (the square in Fig. 2). Though the shortest sulfur-to-sulfur distance is found in p_1 and p_2, these interactions ($\phi=10°$) are located nearly midway between the σ-like and the π-like overlaps of the p_z orbitals. As a consequence, these interactions are

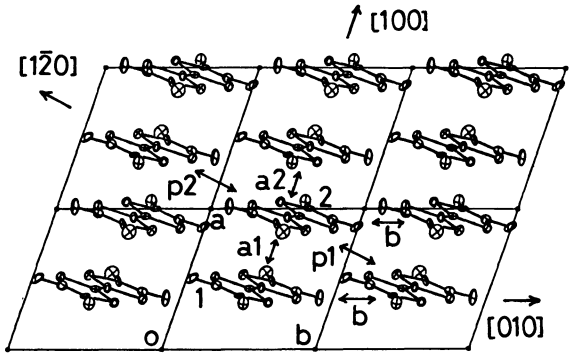

Fig. 5. Intermolecular interactions in $(TMTTF)_2X$.

smaller than the oblique interaction, b, which is close to the peak of the σ-like interaction. Near the region where the overlap crosses zero, the magnitude of the overlap is sensitive to a small variation in the crystal structures. This is also valid for $(TMTSF)_2X$, which is isostructural to $(TMTTF)_2X$. This is the reason why Grant found that the magnitudes of p_1 and p_2 were very sensitive to the kinds of anions, but that other interactions were hardly changed by the anions.[4] The large aniotropy which all the $(TMTSF)_2X$ series compounds show, comes from the large longitudinal interactions, a_1 and a_2, which are scarcely changed by the anions. On the contrary, the difference in the anions, X, causes a small structural variation, which gives rise to the sensitive change of p_1 and p_2, and influences the distortion of the Fermi surface. Therefore, it is possible that the onset of spin-density waves and other instabilities are influenced by the small variation in the crystal structure produced by the anions.

The map of BEDT-TTF in Fig. 3 resembles that of TTF. Figure 4 shows that, in BEDT-TTF, the transverse interactions at $\phi=0°$ and 30° are somewhat enhanced in comparison with those in TTF. The three symbols, a, p, and q, stand for the interactions along [100], [$\bar{1}$02], and [102] respectively in $(BEDT\text{-}TTF)_2ClO_4(C_2H_3Cl_3)_{0.5}$ (Fig. 6). It is worth noting that the overlap along the $\phi=90°$ direction, which exists universally in TTF salts, is not observed in this crystal. As is shown in Fig. 3, p and a are close to the peaks at $\phi=30°$ and $\phi=0°$ respectively. However, q_1, q_2, and q_3 are apart from the peak at $\phi=60°$, $D=1.60$ Å, and are smaller than the other interactions, a and p.

Models of the Energy-band Structures

In actual crystals, the sulfur-to-sulfur distances, $R_{S\text{-}S}$ are not always $R_0=3.80$ Å. However, as is shown in Fig. 7, the overlap integrals change similarly in all the directions as a function of the sufur-to-sulfur distance. Therefore one can estimate the intermolecular overlaps in the actual crystals by using Fig. 7 together with Figs. 2 and 3. The transfer integrals, t, can then be obtained from the relation; $t=E\,S$. Though the best choice of the E value depends on the parameters used for the molecular orbital calculation, we ordinarily use $E=-10$ eV, because it has given realistic values of the transfer integrals for a number of com-

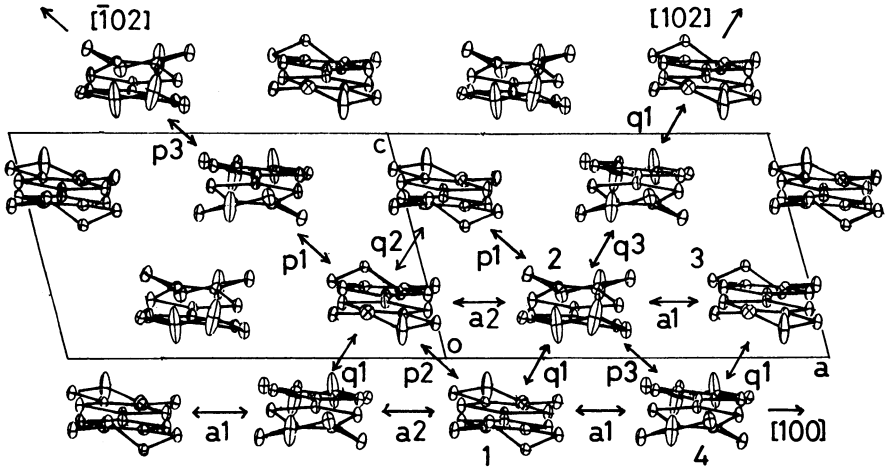

Fig. 6. Intermolecular interactions in $(BEDT\text{-}TTF)_2ClO_4(C_2H_3Cl_3)_{0.5}$.

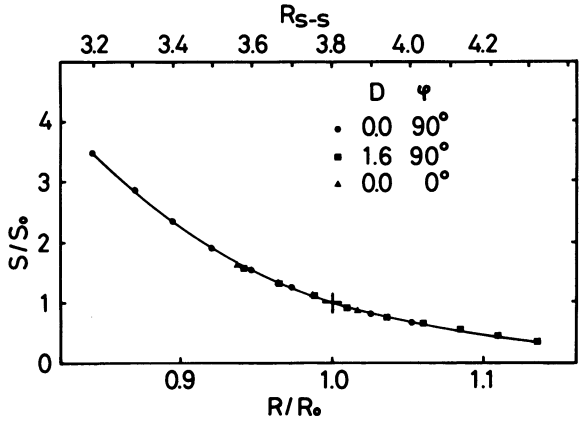

Fig. 7. Relative change of the overlap S as a function of the intermolecular sulfur-to-sulfur distance R, compared with the overlap S_0 at R_0=3.80 Å.

pounds.[9,14,17] When the transfer integrals are estimated, it is easy to obtain the conduction-band structure by the use of the standard tight-binding theory.

From Figs. 2 and 7, the transfer integrals of $(TMTTF)_2X$ were estimated (Table 3(a)). From the standard tight-binding approximation, the matrix elements of the secular equation were;[18]

$$H_{11} = H_{12} = 2t_b \cos kb,$$

$$H_{12} = H_{21}^* = t_{a1} + t_{a2}e^{-ika} + t_{p1}e^{-ikb} + t_{p2}e^{i(kb-ka)}.$$

Solving the resulting quadratic equation, the following dispersion relation was obtained;

$$\varepsilon = 2t_b \cos kb + \Delta^{1/2},$$

$$\Delta = [(t_{a1}+t_{a2})\cos(ka/2) + (t_{p1}+t_{p2})\cos(ka/2-kb)]^2 + [(t_{a1}-t_{a2})\sin(ka/2) + (t_{p1}-t_{p2})\sin(ka/2-kb)]^2.$$

Using this relation, the energy-band structure and the Fermi surface were numerically calculated (Fig. 8). From the stoichiometry, the upper band is exactly half-filled, and the Fermi surface is a plane located around $k_F=\pi/2a$. The deviation from the averaged k_F is about 0.15 π/a. Since, in such a half-filled band, a closed orbit arises only at t_a/t_b=1.0,[19] one may safely conclude that the Fermi surface is a plane.

Table 3. Estimated transfer integrals (in eV)

(a) $(TMTTF)_2X$			(b) $(BEDT\text{-}TTF)_2ClO_4(C_2H_3Cl_3)_{0.5}$		
[100]	t_{a1}	−0.20	[100]	t_{a1}	0.045
	t_{a2}	−0.23		t_{a2}	0.045
[010]	t_b	−0.035	[1̄02]	t_{p1}	−0.060
[12̄0]	t_{p1}	0.020		t_{p2}	−0.060
	t_{p2}	0.007		t_{p3}	−0.060
			[102]	t_{q1}	0.015
				t_{q2}	0.015
				t_{q3}	0.015

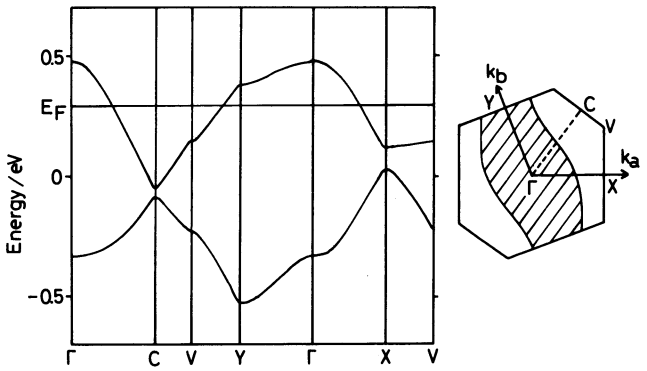

Fig. 8. Band structure and Fermi surface of $(TMTTF)_2X$ calculated by using the transfer integrals in Table 3(a).

Table 3(b) shows the band parameters of $(BEDT\text{-}TTF)_2ClO_4(C_2H_3Cl_3)_{0.5}$ estimated similarly from Figs. 3 and 7. The matrix elements of the secular equation were obtained by reference to Fig. 6;

$$H_{11} = H_{22} = H_{33} = H_{44} = 0,$$

$$H_{12} = H_{21}^* = H_{34}^* = H_{43} = t_{q1} + t_{p1}e^{-ikc},$$

$$H_{13} = H_{31}^* = t_{p2}e^{-ika} + t_{q2}e^{-i(ka+kc)},$$

$$H_{14} = H_{41}^* = H_{23} = H_{32}^* = t_{a1} + t_{a2}e^{-ika},$$

$$H_{24} = H_{42}^* = t_{p3} + t_{q3}e^{ikc}.$$

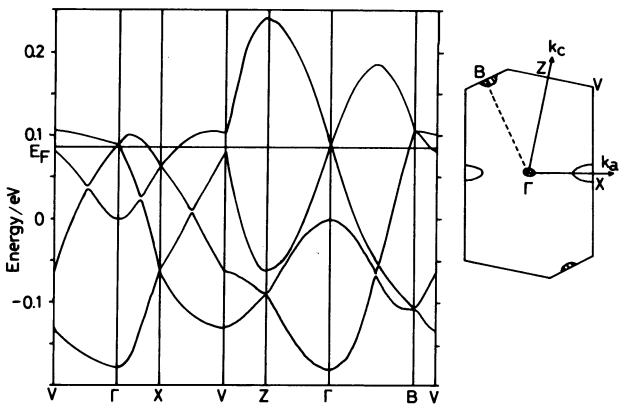

Fig. 9. Band strure and Fermi surface of (BEDT-TTF)$_2$ClO$_4$($C_2H_3Cl_3$)$_{0.5}$ calculated by using the transfer integrals in Table 3(b). The shaded region indicates hole-like part.

By solving the secular equation, the band structure and the Fermi surface were found to be as is shown in Fig. 9. From the stoichiometry of the complex, the conduction band is three-quarters filled. Since the unit cell contains four molecules, the conduction level splits into four bands. Because the alignments along p and q have a fourfold periodicity, if the difference of the overlaps belonging to the same direction, p and q, is very large, the energy gap which is opened between the third and the fourth levels makes the compounds semiconductive. However, since the small difference in the calculated overlaps was not regarded as meaningful because of the qualitative nature of the calculation, the interactions belonging to the same direction were averaged in the model in Table 3(b). Consequently, the resulting band structure is two-dimensional and semimetallic. These results agree with the obwervation of the conductivity and the Drude-like optical reflectance along the two directions.[7,23]

Discussion

The organic superconductors (TMTSF)$_2X$ are isostructural to (TMTTF)$_2$Br. In the present investigation, we did not deal with the calculation of selenium analogs. However, as has already been reported,[10] the band structure of (TMTSF)$_2X$ is qualitatively similar to that of (TMTTF)$_2X$. One of the central points of interest with regard to the band structure of (TMTSF)$_2$-X is whether or not there exists a closed Fermi surface. The only experimental evidence of the closed orbit so far is the observation of the Shubnikov-de Haas resistance.[20] However, as was discussed by Horovitz *et al.*,[21] this observation can be interpreted in terms of the semimetallic electronic states under the spin-density-wave states. Since the large calculated anisotropy agreed with the anisotropy of the conductivity (σ_a/σ_b=300)[22] and the analysis of the optical reflectance (t_b=0.14 eV),[24] we conclude that the Fermi surface at high temperatures is a distorted plane, as is shown in Fig. 8.

Another open question is by what mechanism organic molecules are made to be aligned in the transverse directions, as is found in the actual crystals. Considering a chain of organic donors, the bottom of the conduction band corresponds to the bonding alignment of the element orbitals (HOMO), while the top has an antibonding nature. If this band is partially filled, the wider the band splits (or the stronger the interaction is), the more stable the system becomes by means of the intermolecular bonding, compared with the independent molecules. If the core repulsion is not as dominant as this electrical bonding energy, the orientation giving the maximum of the overlap of the HOMO can be expected to correspond with the most stable molecular alignment. In (BEDT-TTF)$_2$ClO$_4$-($C_2H_3Cl_3$)$_{0.5}$, the interactions, a and p, are close to the peaks of the overlap in Fig. 3. Therefore, the alignment of the molecules along these directions is favorable because of the intermolecular bonding interaction of the HOMO. The absence of the ϕ=90° interaction is probably due to the large core repulsion of the out-of-plane ethylene groups.

The authors wish to thank Dr. Imoto for a part of the program and to Mr. Tajima for his valuable discussions on the band structures. The computations are carried out partly on the HITAC M-200H computer system at the Institute for Molecular Science and partly on the HITAC M-280H computer system at the Computer Center of the University of Tokyo.

References

1) N. Thorup, G. Rindrof, H. Solig, and K. Bechgaard, *Acta Crystallogr., Sect. B*, **37**, 1236 (1981).
2) H. Kobayashi, A. Kobayashi, G. Saito, and H. Inokuchi, *Chem. Lett.*, **1982**, 245.
3) M. -H. Whangbo, W. M. Walsh, Jr., R. C. Haddon, and F. Wudl, *Solid State Commun.*, **43**, 637 (1982).
4) P. M. Grant, *Phys. Rev. B*, **26**, 6888 (1982).
5) T. Mori, A. Kobayashi, Y. Sasaki, and H. Kobayashi, *Chem. Lett.*, **1982**, 1923.
6) C. Minot and S. G. Louie, *Phys. Rev. B*, **26**, 4793 (1982).
7) G. Saito, T. Enoki, K. Toriumi, and H. Inokuchi, *Solid State Commun.*, **42**, 557, (1982).
8) H. Kobayashi, A. Kobayashi, Y. Sasaki, G. Saito, T. Enoki, and H. inokuchi, *J. Am. Chem. Soc.*, **105**, 297 (1983).
9) T. Mori, A. Kobayashi, Y. Sasaki, H. Kobayashi, G. Saito, and H. Inokuchi, *Chem. Lett.*, **1982**, 1963.
10) H. Kobayashi, T. Mori, R. Kato, A. Kobayashi, Y. Sasaki, G. Saito, and H. Inokuchi, *Chem. Lett.*, **1983**, 581.
11) T. J. Kistenmacher, T. E. Phillips, and D. O. Cowan, *Acta Crystallogr., Sect. B*, **30**, 763 (1974).
12) A. J. Berlinsky, J. F. Carolan, and L. Weiler, *Solid State Commun.*, **15**, 795 (1974).
13) J. P. Lowe, *J. Am. Chem. Soc.*, **102**, 1262 (1980), and the references cited therein.
14) T. Mori, unpublished results.
15) B. D. Silverman, *J. Chem. Phys.*, **72**, 5501 (1980).
16) J. L. Gailigne. B. Liautard, S. Peytavin, G. Brun, J. M. Farbe, E. Torreilles, and L. Grial, *Acta Crystallogr., Sect. B*, **34**, 620 (1978).
17) T. Mori, A. Kobayashi, Y. Sasaki, and H. Kobayashi, *Bull. Chem. Soc. Jpn.*, **56**, 3376 (1983).
18) There is some arbitrariness in the choice of the phase factor of the 'basis functions,' which consist of the HOMO on each molecule in a unit cell. In our notation, the origins of all

the MO are taken in common, but conventionally the origins are taken at the center of each molecule. Our notation can easily be transformed to the conventional notation by multiplying a phase factor, for example, $e^{ika/2}$, by the MO of the second molecule in $(TMTTF)_2X$.

19) In a half-filled band, the area of the occupied region is equal to that of the unoccupied region in the first Brillouin zone.

20) J. F. Kwak, J. E. Schirber, R. L. Greene, and E. M. Engler, *Phys. Rev. Lett.*, **46**, 1296 (1981).

21) B. Horovitz, H. Gutfreunt, and M. Weger, *Solid State Commun.*, **39**, 541 (1981).

22) K. Bechgaard, C. S. Jacobsen, K. Mortensen, H. J. Pedersen, and N. Thorup, *Solid State Commun.*, **33**, 1119 (1980).

23) H. Tajima K. Yakushi, H. Kuroda, G. Saito, and H. Inokuchi, *Solid State Commun.*, to be published.

24) J. F. Kwak, *Phys. Rev. B*, **26**. 4789 (1982).